Piotr GAS

AGH University of Science and Technology

Transient Temperature Distribution inside Human Brain during Interstitial Microwave Hyperthermia

Abstract. *This study demonstrates computer simulation of human brain treated with interstitial microwave hyperthermia. A thin coaxial-slot antenna emitting microwaves is the heat source. For simplification, a 2D axisymmetric model is considered. The wave equation for TM wave case and the Pennes bioheat transfer equation for transient-state have been solved with the finite element method. The impact of the time variable on temperature distribution was discussed and the obtained simulation results were presented.*

Streszczenie. *Niniejsza praca pokazuje symulację komputerową mózgu człowieka leczonego przy wykorzystaniu śródmiąższowej hipertermii mikrofalowej. Źródłem ciepła jest cienka współosiowa antena ze szczeliną powietrzną emitująca mikrofale. Równanie falowe dla przypadku fali TM oraz biologiczne równanie przewodnictwa cieplnego określone przez Pennesa dla stanu niestacjonarnego zostały rozwiązane za pomocą metody elementów skończonych. Został przedyskutowany wpływ zmiennej czasowej na rozkład temperatury i przedstawione wyniki symulacji.* ***(Nieustalony rozkład temperatury wewnątrz mózgu człowieka w czasie śródmiąższowej hipertermii mikrofalowej)***

Keywords: interstitial microwave hyperthermia, TM waves, Cole-Cole model, bioheat equation, FEM
Słowa kluczowe: śródmiąższowa hipertermia mikrofalowa, fale TM, model Cola-Cola, biologiczne równanie ciepła, MES

Introduction

Interstitial heating is one of possible ways in hyperthermia treatment, utilizing high frequency needle electrodes, microwave antennas, ultrasound transducers, laser fibre optic conductors, or ferromagnetic rods, seeds or fluids to treat pathological cells located deep within the human body [1]. Thus it can deliver localized and controlled heat exceeding $40^{\circ}\mathrm{C}$ to deep-seated tumors without overheating the surrounding normal tissues. Temperature gradient produced by microwaves can be applied to induce thermonecrosis in cancerous tissues at the distance of 1 to 2 cm around the heat source. It is worth noting that this technique is suitable for tumors less than 5 cm in diameter [2]. Interstitial microwave hyperthermia is widely used clinically in the treatment of recurrent malignancies, in particular such as lung, brain, liver, kidney and breast tumors as well as brain tumors, as reported in [3]. What is more, its uses in combination with radiation therapy and chemotherapy yield more beneficial effects. There are many studies on the treatment of cancer using hyperthermia which demonstrate that this aspect is still important and more research is needed in this matter [4, 5] to make hyperthermia a simpler, safer, more effective and available treatment of cancer. The use of nanotechnology in hyperthermia treatment, e.g. magnetic fluid hyperthermia, which is currently under experimentation, seems particularly promising [6]. The historical background of thermal therapy can be found in [7]. Despite a long history of hyperthermia further investigations in this matter are necessary.

Model geometry and basic equations

The analysed model of the coaxial-slot antenna is shown in Fig. 1 and includes such elements as central conductor, dielectric, outer conductor and a plastic catheter, which performs the protective function for all other elements of the antenna. The air gap with size d is located in the outer conductor. The antenna dimensions are taken from [8] and summarized in Table 1. In fact, the computational area is much larger than it is presented in Fig. 1, and the antenna width does not exceed 2 mm. Due to the axial symmetry of the model cylindrical coordinates r, ϕ, z are used. The 2D model, which includes only half of the antenna structure and the surrounding human brain tissue, is sufficient for analysis.

To derive the basic formulas let us start with the Maxwell's equations in the frequency domain defined as:

$$\nabla \times \mathbf{H} = \mathbf{J} + \mathrm{j}\omega \mathbf{D} \tag{1}$$

$$\nabla \times \mathbf{E} = -\mathrm{j}\omega \mathbf{B} \tag{2}$$

where $\mathbf{E}$ and $\mathbf{H}$ are the electric and magnetic field strengths respectively, ω is the angular frequency of the electromagnetic field and $\mathbf{J}$ is the current density. Moreover, $\mathbf{D}$ and $\mathbf{B}$ are respectively the vectors of electric displacement density and magnetic induction.
After taking into account the Ohm's law in differential form $\mathbf{J} = \sigma\mathbf{E}$ and material dependences $\mathbf{D} = \varepsilon_0\varepsilon_\mathrm{r}\mathbf{E}$ and $\mathbf{B} = \mu_0\mu_\mathrm{r}\mathbf{H}$, and making several transformations of equations (1) and (2), we can derive the following equation describing the field distribution in the complex domain

$$\nabla \times \left[\underline{\varepsilon}_\mathrm{r}^{-1} \nabla \times \mathbf{H} \right] - \varepsilon_0 \mu_0 \mu_\mathrm{r} \omega^2 \mathbf{H} = 0 \tag{3}$$

where ε_0 and μ_0 are the permittivity and permeability of the vacuum, respectively and μ_r is the relative permeability of the medium.

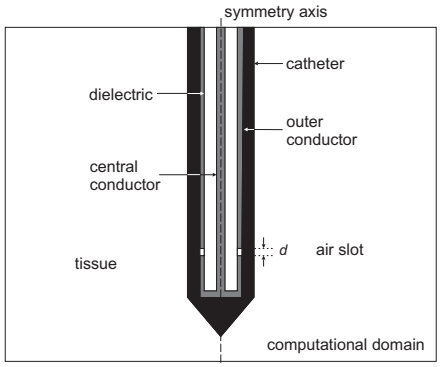

Fig.1. Schematic view of the coaxial-slot antenna located in the human brain

Table 1. Geometrical dimensions of the antenna in [mm]

radius of the central conductor	r_1 = 0.135
inner radius of the outer conductor	r_2 = 0.470
outer radius of the outer conductor	r_3 = 0.595
radius of the catheter	r_4 = 0.895
size of the air slot	d = 1

All the vectors mentioned above are complex. In addition, $\underline{\varepsilon}_r$ is the complex relative permittivity approximated with the Cole-Cole model [9] as follows

$$\underline{\varepsilon}_r(\omega) = \varepsilon_\infty + \frac{\varepsilon_s - \varepsilon_\infty}{1 + (j\omega\tau_0)^{1-\alpha}} - j\frac{\sigma_s}{\omega\varepsilon_0} \tag{4}$$

where ε_∞ is the infinite limit of relative permittivity, ε_s – the static limit of relative permittivity, α – the Cole–Cole parameter, τ_0 – the relaxation time constant [ps] and σ_s – the static conductivity [S/m].

Due to axisymmetric model, transverse magnetic (TM) waves are used and there are no electromagnetic field variations of the magnetic field in the azimuthal direction. Therefore, a magnetic field $\mathbf{H}$ has only the ϕ - component and the wave equation takes the form of scalar equation as

$$\nabla \times \left[\underline{\varepsilon}_r^{-1} \nabla \times H_\phi \right] - \varepsilon_0 \mu_0 \mu_r \omega^2 H_\phi = 0 \tag{5}$$

The full derivation of above equation can be found in [10].

The presented problem models the metallic parts of the antenna using boundary conditions. For all metallic surfaces, the PEC (perfect electric conductor) boundary conditions are set as

$$\mathbf{n} \times \mathbf{E} = 0 \tag{6}$$

The external boundaries of the computational domain, which do not represent a physical boundary have the so-called matched boundary conditions. They make the boundary totally non-reflecting and assume the form

$$\sqrt{\varepsilon_0 \underline{\varepsilon}_r}\ \mathbf{n} \times \mathbf{E} - \sqrt{\mu} H_\phi = -2\sqrt{\mu} H_{\phi 0} \tag{7}$$

where $\boldsymbol{H}_{\phi 0}$ is an input field incident on the antenna given by the formula

$$H_{\phi 0} = \frac{1}{Z r} \sqrt{\frac{Z P_{in}}{\pi \ln(r_2 / r_1)}} \tag{8}$$

In the above equation P_{in} is the total input power in dielectric, while r_1 and r_2 are the dielectric's inner and outer radii, respectively. Moreover, Z signifies the wave impedance of the dielectric which is defined as

$$Z = \frac{Z_0}{\sqrt{\varepsilon_r}} = \sqrt{\frac{\mu_0}{\varepsilon_0 \varepsilon_r}} \tag{9}$$

where Z_0 is the wave impedance of the free space.

The seed point is modelled using a port boundary condition with the power level set to P_{in} at the low-reflection external boundary of the coaxial dielectric cable.

Another basic formulation, the so-called bioheat equation given by Pennes, describes the phenomenon of transport and heat transfer in biological tissues [11]. In the transient analysis it is expressed as

$$\rho C \frac{\partial T}{\partial t} + \nabla(-k \nabla T) = \rho_b C_b \omega_b (T_b - T) + Q_{ext} + Q_{met} \tag{10}$$

where T is the body temperature [K], k – the tissue thermal conductivity [W/(m^2 K)], ρ – the tissue density [kg/m^3], C – the tissue specific heat [J/(kg K)], T_b – the blood vessel temperature [K], ρ_b – the blood density [kg/m^3], ω_b – the blood perfusion rate [1/s], C_b – the blood specific heat [J/(kg K)], t – the time [s].

The described model takes into account both the metabolic heat generation rate Q_{met} [W/m^3] as well as the external heat sources Q_{ext} [W/m^3], which is responsible for the changing of the temperature inside the exposed body according to the equation

$$Q_{ext} = \frac{1}{2}\sigma\, \mathbf{E} \cdot \mathbf{E}^* = \frac{1}{2}\sigma |\mathbf{E}|^2 \tag{11}$$

The Pennes equation (11) requires the specification of both the initial and boundary conditions to be solved. The initial one is as follows

$$T = T_0 = 37°\mathrm{C} \tag{12}$$

which corresponds to the physiological temperature of the human brain. Because the computational domain is limited to a part of the brain tissue, it can be assumed that the heat exchange between parts of the same tissue does not occur and the boundary condition describing this process is

$$\mathbf{n} \cdot (k \nabla T) = 0 \tag{13}$$

where $\mathbf{n}$ is the unit vector normal to the surface.

Computional results

In the analyzed model, the brain tissue and the antenna are considered as homogeneous media with averaged material properties. All physical model parameters of the model are given in Tables 2 – 3. The antenna operates at the frequency $f = 2.45$ GHz and the antenna's input power level is set to $P_{in} = 1$W. What is more, the blood parameters used in the simulation are as follows $T_b = 310.15$ [K], $\rho_b = 1020$ [kg/m^3], $C_b = 3640$ [J/(kg·K)] and $\omega_b = 0.004$ [1/s].

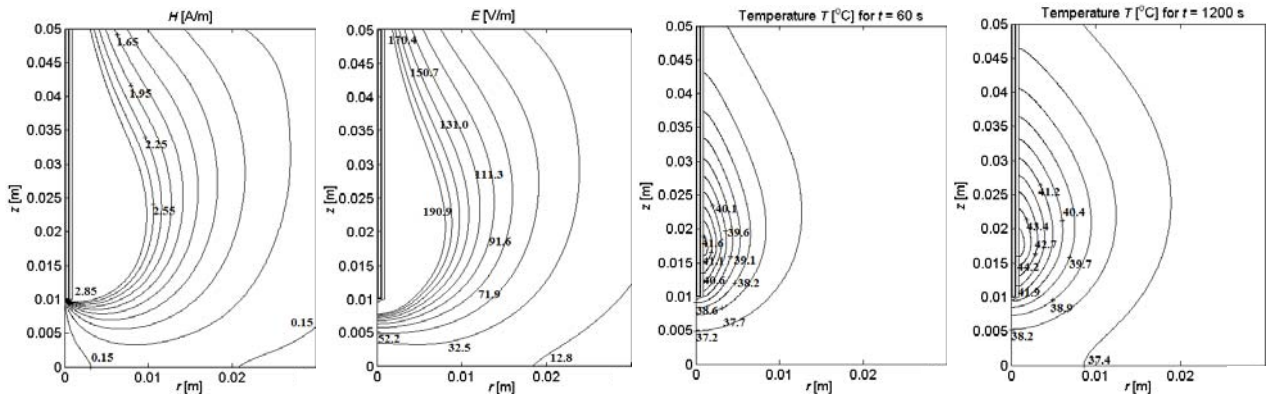

Fig.2. Equipotential lines of the modules of the magnetic and electric field strengths and isotherms in the computational domain after 1 and 20 minutes of microwave hyperthermia treatment, respectively in order from left to right

Table 2. Electrical parameters of the coaxial-slot antenna [8]

	$\mathrm{Re}[\underline{\varepsilon}_r]$	μ_r	σ [S/m]
dielectric	2.03	1	0
catheter	2.60	1	0
air slot	1	1	1

Table 3. Physical parameters of human brain tissue [12, 13]

Tissue	ε_∞	ε_s	τ_0 [ps]	α	σ_s [S/m]
human brain (white matter)	4.0	36	7.958	0.1	0.02

Tissue	k [W/(m·K)]	ρ [kg/m^3]	C [J/(kg·K)]	Q_{met} [W/m^3]
human brain	0.51	1046	3630	300

Equations (5) and (10) with appropriate boundary conditions were solved using the finite element method. The simulation results are summarized in Figures 3 – 5. Contour plots of basic quantities are shown in Fig. 2. Next two illustrations demonstrate the temperature distributions in human brain along two specified paths for different moment of time ranging from 0 to 1200 s (Figures 3 – 4). Time dependent temperature distributions for different distances from the antenna could be seen in Fig. 5.

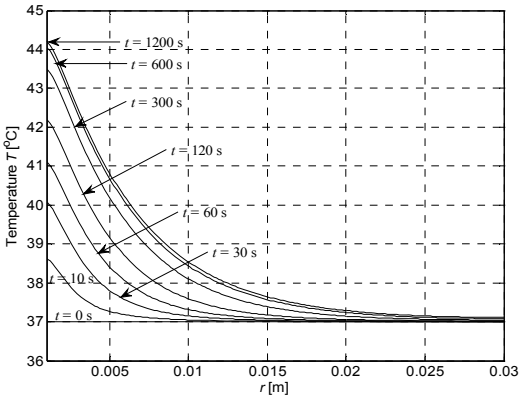

Fig.3. Temperature distribution in the human brain along the path $z = 16$ mm for different moments of time

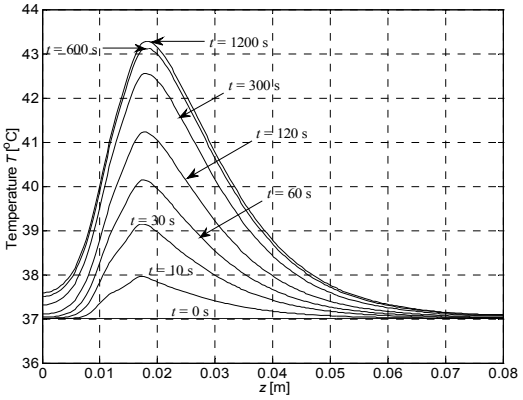

Fig.4. Temperature distribution in the human brain domain along the path $r = 2.5$ mm for different moments of time

Summary

Theoretical study of the transient solution of bioheat equation in interstitial microwave hyperthermia treatment of human brain has been presented. As expected, the tissue temperature decreases rapidly with the distance from the microwave applicator and its largest values occur near the antenna's air gap. Of course when the exposure is longer the temperature observed in the tissue is higher. At the initial moment, the temperature of the human brain is 37°C and after about 10 min it reaches a steady-state at a value close to 44°C. Therapeutic values of the temperature are just 6 mm from the antenna. This range can be easily extended by increasing the antenna's total input power. The described method has been successfully used in medical practice in cancer treatment including brain tumors and its effectiveness increases in combination with radiation and chemotherapy.

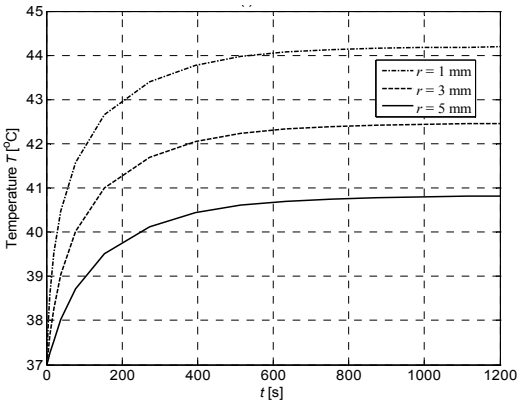

Fig.5. Transient temperature distribution at the points lying along the path $z = 16$ mm for different distances from the antenna

REFERENCES

[1] Habash R.W.Y., Bansal R., Krewski D., Alhafid H.T., Thermal Therapy, Part 2: Hyperthermia Techniques, *Critical Reviews in Biomedical Engineering,* 34 (2006), No. 6, 491-542.

[2] Baronzio G.F., Hager E.D., *Hyperthermia in Cancer Treatment: A Primer*, Landes Bioscience and Springer Science + Business Media, New York (2006).

[3] Kikuchi S., Saito K., Takahashi M., Ito K., Control of heating pattern for interstitial microwave hyperthermia by a coaxial-dipole antenna—aiming at treatment of brain tumor, *Electronics and Communications in Japan (Part I: Communications)*, 90 (2007), 12, 31–38.

[4] Gas P., Temperature inside Tumor as Time Function in RF Hyperthermia, *Electrical Review*, 86 (2010), No. 12, 42-45.

[5] Kurgan E., Gas P., Treatment of Tumors Located in the Human Thigh using RF Hyperthermia, Electrical Review, 87 (2011), No. 12b, 103-106.

[6] Miaskowski A., Sawicki B., Krawczyk A., The use of magnetic nanoparticles in low frequency inductive hyperthermia, *COMPEL: The International Journal for Computation and Mathematics in Electrical and Electronic Engineering*, Vol.31 (2012), Iss. 4, 1096 - 1104.

[7] Gas P., Essential Facts on the History of Hyperthermia and their Connections with Electromedicine, *Electrical Review*, 87 (2011), No. 12b, 37-40.

[8] Saito K., Taniguchi T., Yoshimura H., Ito K., Estimation of SAR Distribution of a Tip-Split Array Applicator for Microwave Coagulation Therapy Using the Finite Element Method, *IEICE Trans. Electronics*, Vol. E84-C (2001), No. 7, 948-954.

[9] Cole K.S., Cole R.H., Dispersion and absorption in dielectrics I: Alternating Current. Characteristics, *J. Chem. Phys.*, 9(1941), 341-351.

[10] Gas P., Temperature Distribution of Human Tissue in Interstitial Microwave Hyperthermia, *Electrical Review*, Vol. 88 (2012), No. 7a, 144-146.

[11] Pennes H.H., Analysis of Tissue and Arterial Blood Temperatures in the Resting Human Forearm, *J. Appl. Physiol.*, 1 (1998), No. 85, 5-34.

[12] Gabriel S., Lau R.W., Gabriel C., The dielectric properties of biological tissues: III. Parametric models for the dielectric spectrum of tissues, *Phys. Med. Biol.*, 41 (1996), 2271-2293.

[13] Mcintosh R. L., Anderson V., A Comprehensive Tissue Properties Database Provided for the Thermal Assessment of a Human at Rest, *Biophysical Reviews and Letters*, 5 (2010), No. 3, 129-151.

***Authors**: mgr inż. Piotr Gas, AGH University of Science and Technology, Department of Electrical and Power Engineering, al. Mickiewicza 30, 30-059 Krakow, E-mail: piotr.gas@agh.edu.pl*